Asymptotic solutions of the Becker-Döring equations

1998 J. Phys. A: Math. Gen. 31 7169

(http://iopscience.iop.org/0305-4470/31/34/018)

J. Phys. A: Math. Gen. **31** (1998) 7169–7189. Printed in the UK PII: S0305-4470(98)94649-2

Asymptotic solutions of the Becker–Döring equations

Jonathan A D Wattis† and John R King‡

Department of Theoretical Mechanics, University of Nottingham, University Park, Nottingham NG7 2RD, UK

Received 27 May 1998

Abstract. We describe the solution of various Becker–Döring models. First, we analyse equilibrium and steady-state solutions, together with the large-time behaviour of solutions for the case of constant monomer concentration. Then we solve a weak fragmentation, constant mass, case by using matched asymptotic expansions. The methods are applied both to the full Becker–Döring equations and to a coarse-grained, or contracted, system. Comparison of the results show good qualitative agreement; all the phenomena present in the full model are reproduced in the contracted system and no anomalous effects are introduced. However, the quantitative agreement depends strongly on the choice of parameter values in the contracted system.

1. Introduction

The Becker–Döring equations were originally proposed in 1935 as a model for nucleation [3]. The model assumes that clusters form by individual particles (monomers) colliding with each other and grow via subsequent collisions with monomers. The fundamental assumption is that clusters do not interact with each other. The collisions are modelled as chemical reactions, leading to a coupled system of ordinary differential equations for the concentrations of clusters of each size. If we denote an r-mer cluster by C_r then the reactions we are concerned with are

$$C_r + C_1 \rightleftharpoons C_{r+1}. \tag{1.1}$$

Note that we allow the mechanism to be reversible; there are thus two reaction rates associated with (1.1) and we denote the forward rates by a_r and the reverse by b_{r+1}, all of which are non-negative. The net flux from clusters of size r to $r+1$ we write as J_r.

In the original work [3] it is assumed that the monomer concentration is fixed. The complete system of equations is then

$$\begin{aligned} \dot{c}_r &= J_{r-1} - J_r \qquad r = 2, 3, 4, \ldots \\ J_r &= a_r c_r c_1 - b_{r+1} c_{r+1} \qquad r = 1, 2, 3, \ldots \end{aligned} \tag{1.2}$$

where c_1 is a prescribed constant. From (1.2) it follows that the total mass (or density)

$$\varrho = \sum_{r=1}^{\infty} r c_r \tag{1.3}$$

† E-mail address: Jonathan.Wattis@nottingham.ac.uk
‡ E-mail address: John.King@nottingham.ac.uk

0305-4470/98/347169+21$19.50

satisfies

$$\dot{\varrho} = J_1 + \sum_{r=1}^{\infty} J_r. \tag{1.4}$$

Later Penrose and Lebowitz [10] suggested a modification whereby the total mass of the system is kept constant, the monomer concentration being allowed to vary. This leads to a more complex system of equations, since the equation for the monomer concentration couples all the other concentrations together in a nonlinear fashion. The governing equations are then

$$\begin{aligned} \dot{c}_1 &= -J_1 - \sum_{r=1}^{\infty} J_r \\ \dot{c}_r &= J_{r-1} - J_r \qquad r = 2, 3, 4, \ldots \\ J_r &= a_r c_r c_1 - b_{r+1} c_{r+1} \qquad r = 1, 2, 3, \ldots . \end{aligned} \tag{1.5}$$

These equations have a rich structure which has, for example, aided Ball *et al* [2] in their existence and uniqueness proofs. Some of this structure is noted at the start of section 4 and is used in constructing the coarse-grained contraction in sections 3 and 5. The density (1.3) is formally conserved by (1.5).

It is the latter system (1.5) that has found greater applicability to physical situations in recent years. The Becker–Döring equations are now applied to a wide range of chemical processes in which phase transitions are involved. These include micelle formation [14, 5], vesicle formation [6], gel-formation and solidification [15]. The aim of this paper is to find asymptotic solutions to the Becker–Döring system of equations in certain limits when the forward and reverse rates are independent of r (though the results are strongly indicative of the behaviour for much more general cases; such generalizations will be presented elsewhere). Due to its wider applicability, we are primarily concerned with (1.5); however, an analysis of the simpler set, (1.2), proves highly instructive and so will be presented first.

The closest related work to ours is that of Slezov *et al* [13], who heuristically identified a succession of stages which the nucleation process passes through, and estimated the duration of each. In this paper we apply systematically the method of matched asymptotic expansions to solve a similar set of governing equations and demonstrate how each asymptotic region matches into its neighbours. We also give the cluster-size distribution at the start and end of each of the key stages of the process. Other previous work includes that of Shneidman [12] who found analytical and numerical approximations to the nucleation waiting time, but relied strongly on steady-state assumptions so that such approaches cannot account for the transient behaviour occurring when a system is initiated from monodisperse conditions, for instance.

Another class of approximate solutions has been provided by use of a coarse-graining approach [5, 15, 6] and we shall give asymptotic solutions to such coarse-grained models also; these will be compared with our results for the full Becker–Döring equations, providing measures of the errors introduced by the coarse-graining approximation procedure. Hounslow *et al* [7, 8] have constructed coarse-grained versions of the general coagulation–fragmentation equations, aiming to find approximate solutions using such a procedure. These solutions were compared with numerical results and some simple analytical checks were performed by analysing the temporal behaviour of the first few moments of the cluster distribution function. Our work has some similarities with this, but we are able to quantify fairly precisely the relationships between our coarse-grained solutions and those of the full system and to indicate means by which optimal choices of parameters in the coarse-grained system may be made.

The rest of the paper is organized as follows. Section 2 contains a description of equilibrium solutions and steady-state solutions of the original Becker–Döring equations (1.2) and of the way in which general solutions approach these special solutions in the large-time limit. In section 3 a coarse-grained version of these equations is derived and the results of section 2 are generalized to cover the new system. Section 4 contains the analysis of the modified Becker–Döring equations (1.5) in the case of a coagulation dominated system, the solution being constructed by matching asymptotic solutions over a series of timescales. These results are generalized to cover the coarse-grain contracted system in section 5. The paper concludes with a discussion of the results in section 6.

2. Original formulation of Becker–Döring

2.1. Formulation

We aim to analyse the original Becker–Döring system (1.2), in which the monomer concentration c_1 is kept fixed, for constant forward and backward rate coefficients, $a_r = a$, $b_r = b$ for all r. Hence

$$\dot{c}_r = J_{r-1} - J_r \qquad J_r = ac_1c_r - bc_{r+1}. \tag{2.1}$$

The initial conditions we are primarily interested in are those in which all concentrations are zero, but the results which follow are valid for any initial conditions which decay sufficiently rapidly with r (see section 2.4.3). We shall make much use of the partition function Q_r, which is related to the rate coefficients via $a_r Q_r = b_{r+1} Q_{r+1}$ with $Q_1 = 1$. The quantity Q_r can be related to the chemical potential of the cluster of size r [5]. In this example the partition function is thus $Q_r = (a/b)^{r-1}$. We introduce the quantity $\theta = ac_1/b$ to simplify many of the subsequent calculations.

In the case of monodisperse initial conditions $c_r(0) = c_1\delta_{r,1}$, use of Laplace transforms in t enables one to find the exact solution to (2.1) as

$$c_r = (r-1)c_1\theta^{(r-1)/2}\int_0^t \frac{\mathrm{e}^{-(ac_1+b)t'} I_{r-1}(2\sqrt{bac_1}t')}{t'}\,\mathrm{d}t' \qquad r \geqslant 2 \tag{2.2}$$

where I_{r-1} is a modified Bessel function. However, rather than directly exploiting (2.2), which it does not seem possible to generalize to the (nonlinear) constant mass case, we shall develop asymptotic methods to investigate the long-time behaviour of the system (2.1). We start by considering the time-independent states which are candidates for the system to approach.

2.2. Equilibrium solution

The most obvious state which may be approached is the equilibrium configuration. This is found by detailed balancing in equations (2.1), which simply means setting the fluxes J_r to zero for all r and solving for the concentrations c_r to give

$$c_r = Q_r c_1^r = \theta^{r-1}c_1. \tag{2.3}$$

Since we require $c_r \to 0$ as $r \to \infty$, we can deduce that (2.3) is relevant only for monomer concentrations $c_1 < b/a$, so that $\theta < 1$. The density (1.3) is then given for $\theta < 1$ by

$$\varrho = \frac{c_1}{(1-\theta)^2}. \tag{2.4}$$

If $\theta \geqslant 1$, we need to look at a wider class of possible attractors to which the system may converge, namely the full class of steady-state solutions.

2.3. Steady-state solution

Here, instead of detailed balancing (i.e. solving $J_r = 0$), we consider all time-independent solutions, which we shall distinguish from the previous case (equilibrium solutions) by calling steady-state solutions. From (2.1) we require that $J_r = J$, independent of r, so that there is a steady flux through the system; the flux out of one aggregation number is exactly balanced by the flux in. In this case, detailed balancing fails. Solving the constant flux condition with a given monomer concentration, we find that

$$c_r = Q_r c_1^r \left[1 - J \sum_{s=1}^{r-1} \frac{1}{a_s Q_s c_1^{s+1}}\right] = c_1 \left[\theta^{r-1} - \frac{J(\theta^r - \theta)}{a c_1^2 (\theta - 1)}\right]. \tag{2.5}$$

If $\theta < 1$ (2.5) implies that $c_r \to -J/b(1-\theta)$ as $r \to \infty$ which, for $J \neq 0$, requires either that $J < 0$, which is unphysical due to there being a flux of mass back from arbitrarily large aggregation numbers, or $c_r < 0$, which is also unphysical. Thus for $c_1 < b/a$, steady-state solutions with $J \neq 0$ are not physically relevant. For $\theta > 1$, however, we have the solution $c_r = c_1$ for all r when $J = c_1(ac_1 - b) > 0$; this value of J corresponds to the weakest possible singularity as $r \to \infty$, all other values of J producing solutions with $c_r \to \pm\infty$ as $r \to \infty$. As $\theta \to 1^+$ we have $J \to 0^+$ and for $\theta = 1$ the two families coincide, this being the bifurcation point.

To summarize the above, as $t \to \infty$ we expect the system to approach the equilibrium solution (2.3) when $c_1 < b/a$ and the steady-state solution $c_r = c_1$ when $c_1 > b/a$, in which case $J = c_1(ac_1 - b)$. This information can be summarized in a bifurcation diagram—see figure 1.

The difference between $\theta < 1$ and $\theta > 1$ can also be seen in the behaviour of the function

$$V = \sum_{r=1}^{\infty} c_r \left(\log\left(\frac{c_r}{Q_r c_1^r}\right) - 1\right) = \sum_{r=1}^{\infty} c_r (\log c_r - (r-1)\log\theta - \log c_1 - 1). \tag{2.6}$$

For $\theta < 1$, the equilibrium solution is a minimizer of V, whereas (2.6) is not bounded below when $\theta > 1$. It can be shown that

$$\frac{\mathrm{d}V}{\mathrm{d}t} = -\sum_{r=1}^{\infty} (ac_r c_1 - bc_{r+1})(\log(ac_r c_1) - \log(bc_{r+1})) \tag{2.7}$$

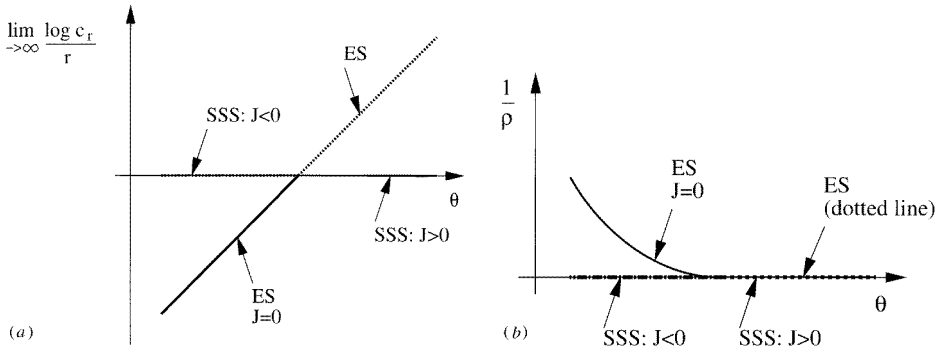

Figure 1. Bifurcation diagrams showing the decay rate of the cluster distribution function and reciprocal of density as functions of θ for equilibrium solutions (ES) and steady-state solutions with $J = c_1(ac_1 - b)$ (SSS). Dotted and broken lines represent unphysical solutions.

so that $\mathrm{d}V/\mathrm{d}t \leqslant 0$ with equality only at equilibrium, and hence V is a Lyapunov function when $\theta < 1$.

Note that, while the steady-state solutions described above are those which are least singular as $r \to \infty$, they do not satisfy $c_r \to 0$ as $r \to \infty$ and consequently do not have finite density. They cannot therefore provide uniformly valid descriptions of the behaviour as $t \to \infty$ and in the next section we use the method of matched asymptotic expansions to complete the picture.

2.4. Large-time asymptotics

2.4.1. Outer solution. For $\theta \leqslant 1$ we expect

$$c_r \sim \theta^{r-1} c_1 \qquad J_r \to 0 \qquad \text{as } t \to \infty \tag{2.8}$$

while for $\theta \geqslant 1$ we anticipate that provided r is not too large

$$c_r \sim c_1 \qquad J_r \sim c_1(ac_1 - b) \qquad \text{as } t \to \infty. \tag{2.9}$$

As already noted, (2.9) is not consistent with the conditions that

$$c_r, J_r \to 0 \qquad \text{as } r \to \infty \tag{2.10}$$

and further regions are needed with r large in order to satisfy (2.10); (2.9) thus provides the leading term in an outer expansion in the limit $r \to \infty$. In fact, (2.8) is not uniform in r either; see section 2.4.4.

We postulate that, for $\theta > 1$, (2.9) is valid for $r/s(t) < 1$, where $s(t) \gg 1$ remains to be determined, and that the outer solution is, to O(1),

$$\begin{aligned} &c_r = c_1 \qquad J_r = c_1(ac_1 - b) \qquad r/s(t) < 1 \\ &c_r = 0 \qquad J_r = 0 \qquad r/s(t) > 1. \end{aligned} \tag{2.11}$$

To find the position of the 'interface', $r = s(t)$, we now construct and solve an equation for the density of the system.

The density of (2.11) satisfies $\varrho \sim \frac{1}{2}c_1 s^2$. Since ϱ satisfies (1.4), it follows, again using (2.11), that $c_1 s\dot{s} = c_1(ac_1 - b)s$ so that

$$s(t) = (ac_1 - b)t \qquad \varrho(t) \sim \tfrac{1}{2}c_1(ac_1 - b)^2 t^2 \qquad \text{as } t \to \infty \tag{2.12}$$

which satisfies, as anticipated, $s(t) \to \infty$ as $t \to \infty$. The function V, defined by (2.6), diverges as $-\frac{1}{2}c_1(ac_1 - b)^2 \log(ac_1/b)t^2$ in this limit.

2.4.2. Transition layer for $\theta > 1$. The transition as $t \to \infty$ between the two regions in (2.11) takes place smoothly, rather than in the abrupt fashion suggested by (2.11). This smoothing occurs over an interior layer close to $r/s = 1$ which we now describe. The leading order behaviour of c_r in this region is described by a continuum formulation of the Becker–Döring equation. Treating r as a continuous variable and expanding the differences in (1.2) in terms of derivatives, we find that to leading order as $t \to \infty$

$$\frac{\partial c}{\partial t} = \frac{1}{2}(ac_1 + b)\frac{\partial^2 c}{\partial r^2} - (ac_1 - b)\frac{\partial c}{\partial r}. \tag{2.13}$$

Since we are here concerned with the large-time asymptotics, we change variables from r to $z = r - s(t)$ in order to focus on the transition region. Writing $c_r(t) = f(z, t)$ and using (2.12) enables the leading order system to be rewritten as

$$\frac{\partial f}{\partial t} = \frac{1}{2}(ac_1 + b)\frac{\partial^2 f}{\partial z^2} \tag{2.14}$$

with matching conditions $f(z,t) \to 0$ as $z \to +\infty$ and $f(z,t) \to c_1$ as $z \to -\infty$. The large-time asymptotics of (2.14) will therefore be governed by the similarity solution $f(z,t) = \frac{1}{2}c_1 \operatorname{erfc}(z/\sqrt{2(ac_1+b)t})$, so that

$$c_r(t) \sim \frac{1}{2}c_1 \operatorname{erfc}\left(\frac{r-(ac_1-b)t}{\sqrt{2(ac_1+b)t}}\right) \qquad \text{as } t \to \infty \qquad \text{with } r-(ac_1-b)t = \mathrm{O}(t^{1/2}). \tag{2.15}$$

The transition layer scaling is thus $(r-s)/s = \mathrm{O}(t^{-1/2})$.

2.4.3. Outer (far-field) region for $\theta > 1$. Earlier, see (2.11), we postulated that the concentrations beyond the transition layer tend to zero as $t \to \infty$. Now we must return to find a leading order representation of the solution in $r/s(t) > 1$ which, in view of the need to match with (2.15), is exponentially small.

In this region we apply the WKB method to the discrete system (2.1), substituting $c_r(t) \sim A(r,t)\mathrm{e}^{w(r,t)}$. At leading order, we then obtain the continuum equation

$$\frac{\partial w}{\partial t} = b\exp\left(\frac{\partial w}{\partial r}\right) - b - ac_1 + ac_1\exp\left(-\frac{\partial w}{\partial r}\right) \tag{2.16}$$

with the correction terms giving

$$\frac{\partial A}{\partial t} = ac_1\left(\frac{1}{2}A\frac{\partial^2 w}{\partial r^2} - \frac{\partial A}{\partial r}\right)\exp\left(-\frac{\partial w}{\partial r}\right) + b\left(\frac{1}{2}A\frac{\partial^2 w}{\partial r^2} + \frac{\partial A}{\partial r}\right)\exp\left(\frac{\partial w}{\partial r}\right). \tag{2.17}$$

To match with (2.15), we require that w take the self-similar form $w(r,t) = tF(\eta)$, $\eta = r/t$, with

$$F(\eta) - \eta F'(\eta) = b\mathrm{e}^{F'(\eta)} - b - ac_1 + ac_1\mathrm{e}^{-F'(\eta)}. \tag{2.18}$$

which is of Clairaut's form (see, for example, [11]). It is the singular solution to (2.18) we require since the general solutions (satisfying $F'' = 0$) correspond to solutions which have exponentially decaying initial concentration profiles; we note the behaviour for exponentially decaying initial data in appendix A. Here, we limit our analysis to initial conditions which decay more rapidly, for which the singular solution is required, namely

$$F(\eta) = \sqrt{\eta^2 + 4ac_1 b} - b - ac_1 - \eta\log\left(\frac{\eta + \sqrt{\eta^2+4ac_1 b}}{2ac_1}\right). \tag{2.19}$$

This provides an alternative derivation of $s(t) = (ac_1 - b)t$, since (2.19) implies that $F = 0$ at $\eta = ac_1 - b$. Using (2.14), we find from (2.17) that $A = G(r/t)/\sqrt{t}$, where $G(r/t)$ depends on the initial conditions and cannot be determined by the large-time asymptotics. This implies the concentrations of clusters beyond the transition layer behave as

$$\log c_r \sim \sqrt{r^2 + 4ac_1 bt^2} - (ac_1+b)t - r\log\left(\frac{r+\sqrt{r^2+4ac_1bt^2}}{2ac_1 t}\right) - \tfrac{1}{2}\log t + \log G(r/t). \tag{2.20}$$

It is easily shown by matching into the transition region that

$$G(\eta) \sim \frac{c_1}{\eta - ac_1 + b}\sqrt{\frac{ac_1+b}{2\pi}} \qquad \text{as } \eta \to (ac_1-b)^+. \tag{2.21}$$

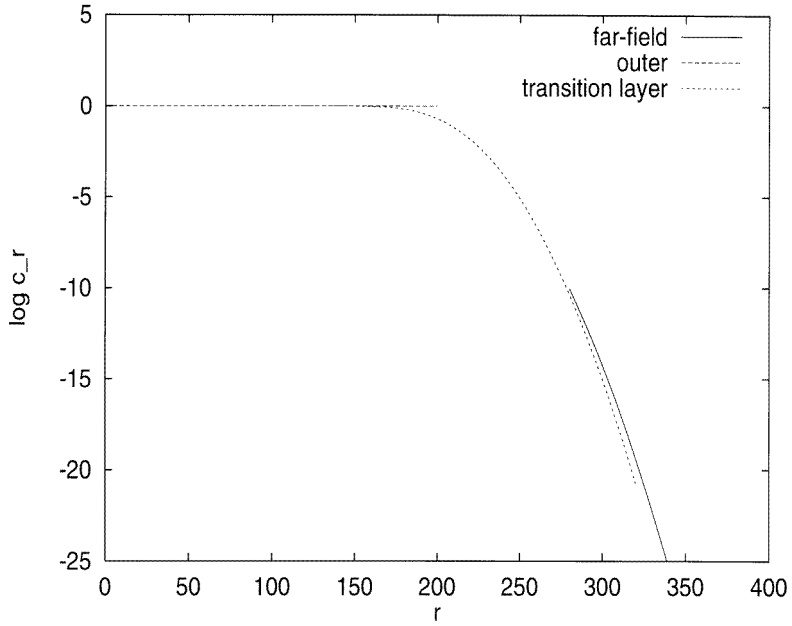

Figure 2. Diagram showing the matching of the leading order outer solution $c_r = c_1$, the transition layer solution (2.15) and the far-field solution (2.19) for the case of $a = 3$, $c_1 = 1$, $b = 1$, $t = 100$.

Figure 2 illustrates the matching of the various regions. We note that for monodisperse initial conditions, the function $G(\eta)$ can be found from an asymptotic expansion of the exact solution (2.2), giving

$$G(\eta) = \frac{\eta\left(\eta + \sqrt{\eta^2 + 4abc_1}\right)}{2a\sqrt{2\pi}(\eta^2 + 4abc_1)^{1/4}\left(\sqrt{\eta^2 + 4abc_1} - b - ac_1\right)}. \tag{2.22}$$

2.4.4. Large-time asymptotics for $\theta \leqslant 1$. While (2.3) represents a finite mass solution for $\theta < 1$, it is nevertheless not uniformly valid as $t \to \infty$ because it decays only algebraically at infinity. Additional regions are once again necessary to describe solutions with more rapidly decaying initial conditions. These can be deduced immediately from the preceeding analysis, since under the transformation $c_r = \theta^{r-1}\phi_r$ the Becker–Döring equations (1.2) become

$$\dot{\phi}_r = H_{r-1} - H_r \qquad H_r = b\phi_r - a\phi_1\phi_{r+1}. \tag{2.23}$$

The role of the forward and backward rates (ac_1 and b respectively) are thus reversed. In particular, if the forward rate is greater than the backward rate in the c-formulation ($ac_1 > b$), the reverse is true in the ϕ-formulation. The substitution thus takes the $\theta < 1$ and $\theta > 1$ cases into one another, with θ being replaced by $1/\theta$; all the results from the $\theta > 1$ case can thus be directly carried over to the present case. For $\theta < 1$, the asymptotic solution

$$\phi_r(t) \sim \frac{1}{2}\phi_1 \operatorname{erfc}\left(\frac{r - (b - a\phi_1)t}{\sqrt{2(b + a\phi_1)t}}\right) \tag{2.24}$$

to (2.23) is equivalent to (2.15) and produces, after 'inversion', the result that for $\theta < 1$

$$c_r(t) \sim \frac{1}{2}\theta^{r-1}c_1 \operatorname{erfc}\left(\frac{r-(b-ac_1)t}{\sqrt{2(ac_1+b)t}}\right) \qquad \text{as } t \to \infty,\ r-(b-ac_1)t = \mathrm{O}(t^{1/2}) \tag{2.25}$$

which clearly matches with (2.3). The special case of $\theta = 1$ is invariant under the transformation and has asymptotic solution

$$c_r(t) \sim c_1 \operatorname{erfc}\left(\frac{r}{2\sqrt{bt}}\right) \qquad \text{as } t \to \infty \qquad \text{for } r = \mathrm{O}(t^{1/2}) \tag{2.26}$$

in this case there being no advection term in (2.13) carrying mass to larger values of r; at large times, the density (1.3) grows linearly, $\varrho \sim bc_1 t$, and the Lyapunov function (2.6) diverges according to

$$V \sim 2c_1\sqrt{bt}\int_0^\infty \operatorname{erfc}(\eta)[\log\operatorname{erfc}(\eta) - 1]\,\mathrm{d}\eta < 0. \tag{2.27}$$

Both therefore grow more slowly than when $\theta > 1$.

Beyond the transition layer there is a further asymptotic region in which the concentrations decay to zero as $r/t \to \infty$. In this regime the concentrations are again governed by (2.20), $G(\eta)$ depending on the initial concentrations. The far-field structure is thus the same for all θ. By matching into the transition region, we see that for $\theta \leqslant 1$

$$G(\eta) \sim \frac{c_1}{\theta(\eta - b + ac_1)}\sqrt{\frac{ac_1+b}{2\pi}} \qquad \text{as } \eta \to (b-ac_1)^+. \tag{2.28}$$

Equation (2.22) again applies in the case of monodisperse initial conditions.

3. Coarse-grained system with constant monomer

3.1. Formulation

A coarse-grained contraction of the equations (1.2) relies on grouping clusters of similar sizes together and eliminating all but one of the variables that describe their concentrations. The one we choose to keep is that for the largest cluster size in the group. Since the monomer concentration is a parameter, this is not taken to be part of the averaging procedure and we define $x_1 := c_1$. The first stage of the process is to decide how to split up all the aggregation numbers into groupings. Here, we shall lump the same number, λ, of different cluster sizes together into each grouping. For example, if we choose $\lambda = 4$, then x_2 is used in place of the concentrations previously denoted c_2, c_3, c_4, c_5, and x_3 in place of c_6, c_7, c_8, c_9, and so on. The procedure is perhaps better shown diagramatically:

$$\underbrace{c_1}_{x_1}\underbrace{c_2\ldots c_{\lambda+1}}_{x_2}\underbrace{c_{\lambda+2}\ldots c_{2\lambda+1}}_{x_3}\cdots\underbrace{c_{(p-2)\lambda+2}\ldots c_{(p-1)\lambda+1}}_{x_p}\underbrace{c_{(p-1)\lambda+2}\ldots c_{p\lambda+1}}_{x_{p+1}}\cdots.$$

In general, we take $x_p = c_{(p-1)\lambda+1}$ as representative of all the concentrations from $c_{(p-2)\lambda+2}$ to $c_{(p-1)\lambda+1}$.

To define a flux from the grouping x_p to x_{p+1} we eliminate $c_{(p-1)\lambda+2}$ to $c_{p\lambda}$ between the fluxes

$$\begin{aligned}
J_{(p-1)\lambda+1} &= a_{(p-1)\lambda+1}c_{(p-1)\lambda+1}c_1 - b_{(p-1)\lambda+2}c_{(p-1)\lambda+2}\\
J_{(p-1)\lambda+2} &= a_{(p-1)\lambda+2}c_{(p-1)\lambda+2}c_1 - b_{(p-1)\lambda+3}c_{(p-1)\lambda+3}\\
&\ \ \vdots \quad \vdots \qquad \vdots \qquad\qquad \vdots\\
J_{p\lambda} &= a_{p\lambda}c_{p\lambda}c_1 - b_{p\lambda+1}c_{p\lambda+1}
\end{aligned} \tag{3.1}$$

leaving

$$\left(\prod_{n=2}^{\lambda+1} b_{(p-1)\lambda+n}\right)\sum_{k=1}^{\lambda}\frac{c_1^{\lambda-k}J_{(p-1)\lambda+k}}{a_{(p-1)\lambda+k}Q_{(p-1)\lambda+k}} = \left(\prod_{n=1}^{\lambda} a_{(p-1)\lambda+n}\right)c_{(p-1)\lambda+1}c_1^{\lambda} - \left(\prod_{n=2}^{\lambda+1} b_{(p-1)\lambda+n}\right)c_{p\lambda+1}. \tag{3.2}$$

In (3.2) we now replace $c_{(p-1)\lambda+1}$ by x_p and $c_{p\lambda+1}$ by x_{p+1}; we then use (3.2) to define the flux from x_p to x_{p+1}. The equations we postulate for the $x_p(t)$ and the new fluxes $L_p(t)$ are then

$$\begin{aligned} &\dot{x}_p = \frac{L_{p-1}-L_p}{\lambda}, \ (p \geqslant 3) \qquad L_p = \lambda(\alpha_p x_1^{\lambda} x_p - \beta_{p+1}x_{p+1}), \ (p \geqslant 2) \\ &\dot{x}_2 = L_1 - \frac{L_2}{\lambda} \qquad L_1 = \alpha_1 x_1^{\lambda+1} - \beta_2 x_2 \end{aligned} \tag{3.3}$$

where α_p, β_p are the rescaled forward and backward rate coefficients defined from (3.2) by

$$\alpha_p = \prod_{n=1}^{\lambda} a_{(p-1)\lambda+n} \qquad \beta_{p+1} = \prod_{n=2}^{\lambda+1} b_{(p-1)\lambda+n}. \tag{3.4}$$

We have defined the fluxes L_p for $p \geqslant 2$ in a slightly different way to that presented in [5] in order that the flux L_p represents the quantity of material being moved from clusters of size $\Lambda_p := (p-1)\lambda + 1$ to those of size Λ_{p+1}. The flux L_1 has a separate definition omitting the multiplicative λ. However, when all the L_p variables are eliminated from (3.3) the same system is obtained as in [6]. Constant rates $a_r = a$, $b_r = b$ in the full model correspond to constant rates $\alpha_p = a^{\lambda}$, $\beta_p = b^{\lambda}$ in the reduced model (3.3), so that $\alpha x_1^{\lambda}/\beta = (ac_1/b)^{\lambda} = \theta^{\lambda}$. The partition function Q_r is now sampled only at certain cluster sizes, $Q_{(p-1)\lambda+1} = (\alpha/\beta)^{p-1}$. The coarse-graining procedure is generalized in [6, 15].

Equations (3.3) with constant coefficients $\alpha_p = \alpha$ and $\beta_p = \beta$ are identical to (2.1) (with α, β and x_1^{λ} replacing a, b and c_1 respectively and with L_1 replacing J_1 and L_p/λ replacing J_p for $p \geqslant 2$). In the remainder of this section we assess the validity of the coarse-graining procedure by comparing the large-time behaviour of (3.3) to that of (2.1); the former can immediately be deduced from the latter.

3.2. Equilibrium solution

The equilibrium solution to (3.3) is

$$x_p = Q_{(p-1)\lambda+1}x_1^{(p-1)\lambda+1} = \theta^{(p-1)\lambda}x_1 \tag{3.5}$$

so, at equilibrium $x_p = c_{(p-1)\lambda+1}$. This solution is relevant only for $\theta < 1$.

Since x_p corresponds to $c_{(p-1)\lambda+1}$, we assign a representative mass of $(p-1)\lambda + 1$ to the cluster denoted x_p. The appropriate definition of density for the contracted system is then

$$\mu := \sum_{p=1}^{\infty}[(p-1)\lambda + 1]x_p. \tag{3.6}$$

An extra factor of λ appears in the evolution equation for μ due to the fact that λ monomers need to be added to take a cluster from x_p to x_{p+1}; in place of (1.4), it follows from (3.3) that we have

$$\dot{\mu} = \lambda L_1 + \sum_{p=1}^{\infty} L_p. \tag{3.7}$$

At equilibrium (3.6) can be evaluated to give

$$\mu = \frac{x_1[\,1 + (\lambda - 1)\theta^\lambda]}{(1 - \theta^\lambda)^2}. \tag{3.8}$$

By comparing this with (2.4) we obtain a measure of the error induced by the contraction procedure. The key point, however, is that the coarse-graining does not affect the nature of the equilibrium solution; density still diverges if $\theta \geqslant 1$ and is finite if $\theta < 1$, giving the same regions of physical and unphysical behaviour as for the uncontracted case, the equilibrium solution again providing the large-time behaviour for $\theta < 1$.

3.3. Steady-state solution

As with the original formulation (2.1), there is a one-parameter family of steady-state solutions given by constant flux, $L_p(t) = L$ for all $p \geqslant 2$ and $L_1(t) = L/\lambda$. For $L = \lambda x_1(\alpha x_1^\lambda - \beta)$, the solution is $x_p = x_1$ for all p and, for $\theta \geqslant 1$, this steady-state solution provides the large-time behaviour. Thus the bifurcation diagram for the reduced system (3.3) is qualitatively identical to that for the full system (see figure 1).

The ratio of the fluxes of the steady-state solution in the reduced system to that in the original system is

$$\frac{L}{J} = \frac{\lambda b^{\lambda-1}(\theta^\lambda - 1)}{(\theta - 1)}. \tag{3.9}$$

Thus the steady-state flux in the contracted system (3.3) is in general not the same as that in the original system (2.1). However, there is a degree of arbitrariness in the definitions of the reaction rates and timescales in the contracted system; specifically, a simple rescaling of time $t = \hat{t}/t_0$ in the original system (2.1) alters the values of a and b to $\hat{a} = a/t_0$, $\hat{b} = b/t_0$ (leaving θ unchanged); in view of (3.4), these changes in a and b correspond to rescaling t in the coarse-grained system by a different factor, namely t_0^λ. We can thus make the steady-state fluxes in both systems equal by formulating the original problem on a timescale which forces the right-hand side of (3.9) to be unity; this is achieved by choosing

$$t_0 = b\left[\frac{\lambda(\theta^\lambda - 1)}{(\theta - 1)}\right]^{1/(\lambda-1)}. \tag{3.10}$$

These comments indicate a significant deficiency in the coarse-graining procedure, in that it does not in general preserve the timescales of the original system. However, the qualitative behaviour is similar to that of the uncontracted system and judicious choices of scaling can lead to good agreement in the quantitative behaviour also.

3.4. Large-time asymptotics

Having seen that the structure and form of the time-independent solutions of the Becker–Döring equations are largely unaltered by the coarse-graining contraction procedure, we now examine the large-time kinetics.

For $\theta > 1$, our solution at O(1) comprises (cf (2.11))

$$\begin{aligned} &x_p = x_1 \qquad L_p = \lambda x_1(\alpha x_1^\lambda - \beta) \qquad p/\sigma(t) < 1 \\ &x_p = 0 \qquad L_p = 0 \qquad p/\sigma(t) > 1 \end{aligned} \tag{3.11}$$

with (cf (2.12))

$$\sigma(t) = (\alpha x_1^\lambda - \beta)t \qquad \mu(t) \sim \tfrac{1}{2}\lambda x_1(\alpha x_1^\lambda - \beta)^2 t^2 \qquad \text{as } t \to \infty. \tag{3.12}$$

The ratio of the translational speed of the transition region in the contracted set of equations (3.3) to that of the full system (2.1) is

$$\frac{\lambda\dot{\sigma}}{\dot{s}} = \frac{\lambda b^{\lambda-1}(\theta^{\lambda}-1)}{(\theta-1)}. \tag{3.13}$$

The λ is included on the left-hand side because a unit increment in p corresponds to an increment of λ in the aggregation number r. The right-hand side of the expression (3.13) is identical to that of (3.9); thus by rescaling time by (3.10) both the flux ratio and speed ratio can be corrected.

4. Constant density systems

4.1. Introduction

In this section we aim to construct asymptotic solutions to the density conserving version of the Becker–Döring equations (1.5) proposed by Penrose and Lebowitz [10] in a special case. The case we shall examine is that in which the forward reaction dominates the reverse. We shall use matched asymptotic expansions to identify the various stages that the cluster-formation process passes through and to determine the leading order solutions.

In this formulation the monomer concentration is allowed to vary ($c_1 = c_1(t)$), but the density (1.3) is fixed, so the monomer concentration satisfies the first of (1.5). Conservation of density is the first of four properties of the system of equations (1.5) that we shall note. Other important properties are the existence of a Lyapunov function (2.6), which corresponds to the free energy of the system, the existence of a unique equilibrium solution, $c_r = Q_r c_1^r$ and, finally, the weak form

$$\sum_{r=1}^{\infty} g_r \dot{c}_r = \sum_{r=1}^{\infty} (g_{r+1} - g_r - g_1) J_r \tag{4.1}$$

where $\{g_r\}_{r=1}^{\infty}$ is an arbitrary sequence satisfying $a_r(g_{r+1} - g_r) = \mathrm{O}(g_r)$ as $r \to \infty$ (see Ball *et al* [2] for detailed analysis using this weak form). While we shall not make direct use of (4.1), we will ensure that a similar set of identities exists after the coarse-graining contraction procedure has been applied.

For any density, there is a unique equilibrium value of the monomer concentration c_1, determined by (2.4) and being such that $\theta < 1$ for any finite ϱ (in fact, $\theta = (b + 2a\varrho - (b^2 + 4ab\varrho)^{1/2})/2a\varrho$), and the large-time behaviour follows the approach to equilibrium described in section 2.4.4. In this case the speed of propagation of the transition region is best found from the matching with the WKB solution in the far-field region, again giving $s(t) = (b - ac_1)t$. When the forward reaction dominates the reverse it is possible to make significant further analytical progress in understanding the time-dependent problem, and the remainder of this section is devoted to this coagulation dominated case. We take $a_r = a$, with $a = 1$ without loss of generality, and $b_r = b = \varepsilon$ with $\varepsilon \ll 1$, so that the equations we analyse are

$$\dot{c}_1 = -J_1 - \sum_{r=1}^{\infty} J_r \qquad \dot{c}_r = J_{r-1} - J_r \qquad (r \geqslant 2) \qquad J_r = c_r c_1 - \varepsilon c_{r+1}. \tag{4.2}$$

We have $\theta \sim 1 - \sqrt{\varepsilon/\varrho}$ as $\varepsilon \to 0$. For simplicity monodisperse initial conditions will be assumed ($c_1 = \varrho$, $c_r = 0$ for $r \geqslant 2$), though the analysis readily generalizes. Four distinct timescales need investigation.

4.2. $t = O(1)$

The first timescale is more easily analysed by a transformation of both the time variable and the dependent variables. We substitute $c_r(t) = c_1(t)\xi_r(\tau)$, so that $\xi_1 = 1$. The new time variable τ is defined by

$$\tau = \int_0^t c_1(s)\,\mathrm{d}s. \tag{4.3}$$

This transforms equations (4.2) to, at leading order in ε (the fragmentation terms being negligible),

$$\frac{\mathrm{d}\xi_r}{\mathrm{d}\tau} = \xi_{r-1} + \Xi\xi_r \qquad r \geqslant 2 \tag{4.4}$$

where $\Xi(\tau) = \sum_{k=1}^{\infty} \xi_k(\tau)$, which from (4.4) satisfies

$$\frac{\mathrm{d}\Xi}{\mathrm{d}\tau} = \Xi^2 \tag{4.5}$$

so that $\Xi = (1-\tau)^{-1}$. Equations (4.4) can then be successively solved to give

$$\xi_r = \frac{\tau^{r-1}(r-\tau)}{r!(1-\tau)}. \tag{4.6}$$

The equation for c_1 from (4.2) now reduces to

$$\frac{\mathrm{d}c_1}{\mathrm{d}\tau} = -(1+\Xi)c_1 \tag{4.7}$$

and gives

$$c_1 = \varrho(1-\tau)\mathrm{e}^{-\tau} \tag{4.8}$$

as found by Brilliantov and Krapivsky [4]. Thus the leading order relationship between t and τ is

$$\varrho t = e[E_1(1-\tau) - E_1(1)] \tag{4.9}$$

where $E_1(z)$ is the exponential integral defined in equation (5.1.1) of Abramowitz and Stegun [1].

It is not hard to see from this solution (which gives the exact solution to the pure coagulation problem) that a new timescale is needed when τ approaches unity, and in this limit $t \to \infty$. The fragmentation terms in the kinetic equations (4.2) become significant when $c_1 \sim \varepsilon$, so we can deduce that the required new scalings are $\tau = 1 + \varepsilon\tau_2$, $c_1 = \varepsilon C_1$. Reverting to the original variables $c_r = \xi_r c_1$ then, since

$$c_r = \frac{\varrho\tau^{r-1}(r-\tau)\mathrm{e}^{-\tau}}{r!} \tag{4.10}$$

we have $c_r \sim \varrho(r-1)/er!$ as $\tau \to 1$. (4.9) is equivalent to

$$\frac{\varrho t}{e} = -E_1(1) - \gamma - \log(1-\tau) - \sum_{n=1}^{\infty} \frac{(\tau-1)^n}{nn!} \qquad \text{for } \tau < 1 \tag{4.11}$$

which implies that $t = (e/\varrho)\log(1/\varepsilon) + \mathrm{O}(1)$ for $\tau_2 = \mathrm{O}(1)$, and we define $t_2 = t - (e/\varrho)\log(1/\varepsilon)$.

4.3. $t = (e/\varrho)log(1/\varepsilon) + O(1)$

The leading order equations on the timescale $t_2 = \mathrm{O}(1)$ are

$$\dot{C}_1 = c_2 + \frac{\varrho}{e} - \frac{\varrho}{e}C_1 \qquad \dot{c}_r = 0 \qquad \text{for } r \geqslant 2. \tag{4.12}$$

Matching with the previous timescaling we therefore have, to leading order,

$$c_r = \frac{\varrho(r-1)}{er!} \qquad \text{for } r \geqslant 2 \tag{4.13}$$

with the scaled monomer concentration given by

$$C_1 = \tfrac{3}{2} + \varrho \exp(-\gamma - 1 - E_1(1) - \varrho t_2/e) \tag{4.14}$$

again matching with the previous timescale as $t_2 \to -\infty$ using (4.8) and (4.11).

Rather than tending to zero, as would occur in the pure coagulation case, the monomer concentration thus tends over this timescale to an $\mathrm{O}(\varepsilon)$ constant; all the other concentrations are constant to leading order. Since these values do not correspond to the equilibrium configuration, it is clear that at least one further timescale is needed in which other terms enter the leading order rate equations.

4.4. $t = O(1/\varepsilon)$

In order to obtain the required balance in the dimer equation, the next timescale can be identified as $t_3 = \varepsilon t$, giving

$$\begin{aligned}
\varepsilon\frac{\mathrm{d}C_1}{\mathrm{d}t_3} &= c_2 - C_1\sum_{r=2}^{\infty} c_r + \sum_{r=1}^{\infty} c_{r+1} - \varepsilon C_1^2 \\
\frac{\mathrm{d}c_2}{\mathrm{d}t_3} &= \varepsilon C_1^2 - C_1c_2 - c_2 + c_3 \\
\frac{\mathrm{d}c_r}{\mathrm{d}t_3} &= C_1c_{r-1} - C_1c_r - c_r + c_{r+1} \qquad r \geqslant 3
\end{aligned} \tag{4.15}$$

with leading order initial conditions determined from (4.13), (4.14), as

$$\text{at } t_3 = 0 \qquad C_1 = \tfrac{3}{2} \qquad c_r = \frac{\varrho(r-1)}{er!}. \tag{4.16}$$

At leading order we therefore have

$$\begin{aligned}
C_1(t_3) &= 1 + \frac{c_2(t_3)}{\sum_{r=2}^{\infty} c_r(t_3)} \\
\frac{\mathrm{d}c_2}{\mathrm{d}t_3} &= -C_1c_2 - c_2 + c_3
\end{aligned} \tag{4.17}$$

and (4.15).

It does not seem possible to solve the equations for the remaining variables c_r, but we can outline the behaviour as $t_3 \to \infty$, which is determined by the continuum limit of (4.15). As we shall see, $c_2/\sum_{r=2}^{\infty} c_r \to 0$ as $t_3 \to +\infty$ (see (4.19)), so that $C_1(t_3) \to 1$. The large-time limit of (4.15) is then simply

$$\frac{\partial c}{\partial t_3} = \frac{\partial^2 c}{\partial r^2} \tag{4.18}$$

which applies for $r = \mathrm{O}(t_3^{1/2})$ and has as its large-time behaviour the mass-preserving similarity solution

$$c(r, t_3) \sim \frac{\varrho r \mathrm{e}^{-r^2/4t_3}}{2\sqrt{\pi} t_3^{3/2}} \qquad \text{as } t_3 \to \infty \qquad \text{with } r = \mathrm{O}(t_3^{1/2}) \tag{4.19}$$

since the boundary condition $c \to 0$ as $r/t_3^{1/2} \to 0$ is required to match; the density condition

$$\int_0^\infty r c(r, t_3)\, \mathrm{d}r \sim \varrho \tag{4.20}$$

has been imposed. From (4.15) and (4.19), we have $c_r \sim \varrho(r-1)/2\sqrt{\pi} t_3^{3/2}$ as $t \to +\infty$ for $r = \mathrm{O}(1)$ with $r \geqslant 2$.

4.5. $t = O(1/\varepsilon^2)$

We see from (4.19) that the initial mass has spread out into a smooth, slowly varying (in r) distribution, with the concentrations c_r ($r \geqslant 2$) all decaying to zero as $t_3 \to \infty$. However, since this still does not converge to the equilibrium solution as $t_3 \to \infty$, a further scaling is required, the continuum formulation of the problem still being applicable in the outer region.

The monomer concentration has, to leading order, reached its equilibrium value $c_1 = \varepsilon$, and we shall need the second term in its expansion, $c_1 \sim \varepsilon + \varepsilon^{3/2} D_1$. Introducing the scalings $t_4 = \varepsilon^2 t$, $r_4 = \varepsilon^{1/2} r$, and $c_r = \varepsilon C(r_4, t_4)$, we find

$$\frac{\partial C}{\partial t_4} = \frac{\partial^2 C}{\partial r_4^2} - D_1(t_4) \frac{\partial C}{\partial r_4} \tag{4.21}$$

for $r_4 = \mathrm{O}(1)$; (4.21) governs the outer solution. For $r = \mathrm{O}(1)$ we must return to the discrete Becker–Döring equations (4.2) and use the current scalings (whereby $c_r = \varepsilon C_r$) to give the inner solution. To leading order, (4.2) is then $C_{r-1} - 2C_r + C_{r+1} = 0$, and matching thus gives $C_r = 1$ for all r. The matching condition on the outer problem (4.21) is therefore $C = 1$ at $r_4 = 0$; moreover (4.19) implies that the appropriate initial condition is $C = -\varrho\delta'(r_4)$ at $t_4 = 0$. Conservation of mass (4.20) together with (4.21) gives

$$D_1(t_4) = -1 \Big/ \int_0^\infty C(r_4, t_4)\, \mathrm{d}r_4. \tag{4.22}$$

The time-dependent problem (4.21) cannot be solved explicitly due to the (novel) non-local nonlinearity caused by the presence of $D_1(t_4)$ (see (4.22)), but the large-time behaviour is given by the time-independent solution

$$C = \exp(-r_4/\sqrt{\varrho}) \qquad D_1 = -1/\sqrt{\varrho} \tag{4.23}$$

which is in leading order agreement for $r_4 = \mathrm{O}(1)$ with the exact equilibrium solution (2.3) with $\theta = 1 - \sqrt{\varepsilon/\varrho} + \mathrm{O}(\varepsilon)$.

In summary, the solution thus proceeds through four timescales. During the first the monomers aggregate until their concentration becomes small. Over the second the monomer concentration stabilizes, and the other concentrations are constant. This timescale is shifted from the first by an amount $(e/\varrho)\log(1/\varepsilon)$, which can be interpreted as a waiting time before the cluster distribution starts to contain appreciable numbers of larger clusters. During the third timescale ($t = \mathrm{O}(1/\varepsilon)$), processes akin to diffusion in r-space occur, the distribution evolving into the single-humped function (4.19) with a peak at $r = \sqrt{2\varepsilon t}$. This shape is seen in other applications with different governing equations, for example it is qualitatively

similar to that found by Hounslow *et al* [7, 8], in studies of pure aggregation in the full Smoluchowskii equations with a constant kernel. Finally, the equilibrium configuration is approached over the timescale $t = \mathrm{O}(1/\varepsilon^2)$, with all concentrations small and with the profile reverting to a monotonically decaying distribution.

5. Contracted constant density system

5.1. Introduction

The coarse-grained contraction of the constant density version of the Becker–Döring equations was originally given in [5]; it constitutes a modification to (3.3) whereby we have the additional equation

$$\dot{x}_1 = -\lambda L_1 - \sum_{p=1}^{\infty} L_p \tag{5.1}$$

for the monomer concentration. The system (3.3), (5.1) then possesses the four previously noted properties of the uncontracted system (1.5), namely (a) a unique equilibrium solution $x_p = Q_{(p-1)\lambda+1} x_1^{(p-1)\lambda+1}$, (b) a conserved quantity (the density) defined by the modified definition (3.6), (c) a Lyapunov function $V = \sum_{p=1}^{\infty} x_p(\log(x_p/Q_{(p-1)\lambda+1}) - 1)$, and (d) a modified weak form

$$\sum_{p=1}^{\infty} g_p \dot{x}_p = (g_2 - (\lambda+1)g_1)L_1 + \sum_{p=2}^{\infty} \left(\frac{g_{p+1} - g_p}{\lambda} - g_1 \right) L_p. \tag{5.2}$$

In the remainder of this section, we solve the coagulation dominated limit of these equations, namely

$$\begin{aligned} &\dot{x}_1 = -\lambda L_1 - \sum_{p=1}^{\infty} L_p \qquad \dot{x}_2 = L_1 - \frac{L_2}{\lambda} \qquad L_1 = x_1^{\lambda+1} - \varepsilon^{\lambda} x_2 \\ &\dot{x}_p = \frac{L_{p-1} - L_p}{\lambda}, \ (p \geqslant 3) \qquad L_p = \lambda(x_1^{\lambda} x_p - \varepsilon^{\lambda} x_{p+1}), \ (p \geqslant 2) \end{aligned} \tag{5.3}$$

and show that its solution structure is the same as that for the full system (4.2), demonstrating that the coarse-graining approximation procedure does not introduce spurious behaviour into the reduced system of equations.

5.2. $t = O(1)$

We follow the same procedure as in section 4. First, we substitute $x_p(t) = x_1(t)\zeta_p(\tau)$ where the new time variable is defined by

$$\tau = \int_0^t x_1^{\lambda}(s)\,\mathrm{d}s. \tag{5.4}$$

Thus to leading order (5.3) becomes

$$\frac{\mathrm{d}\zeta_p}{\mathrm{d}\tau} = \zeta_{p-1} + \lambda \Upsilon \zeta_p \tag{5.5}$$

where $\Upsilon = \sum_{k=1}^{\infty} \zeta_k$ satisfies

$$\frac{\mathrm{d}\Upsilon}{\mathrm{d}\tau} = \lambda \Upsilon^2 - (\lambda - 1)\Upsilon \tag{5.6}$$

which contains an additional term not present in the uncontracted case. Imposing $\Upsilon(0) = 1$ gives for $\lambda > 1$

$$\Upsilon(\tau) = \frac{\lambda - 1}{\lambda - \mathrm{e}^{(\lambda-1)\tau}}. \tag{5.7}$$

Using an integrating factor to solve (5.5) sequentially, we find

$$\zeta_p(\tau) = \frac{1}{\lambda \mathrm{e}^{-(\lambda-1)\tau} - 1}\left[\sum_{k=0}^{p-2} \frac{\lambda(-1)^{k+p}\tau^k}{(\lambda-1)^{p-k-1}k!} - \frac{\tau^{p-1}}{(p-1)!} - \frac{\lambda(-1)^p \mathrm{e}^{-(\lambda-1)\tau}}{(\lambda-1)^{p-1}}\right] \quad \text{for } p \geqslant 2. \tag{5.8}$$

The equation for x_1, namely

$$\frac{\mathrm{d}x_1}{\mathrm{d}\tau} = -(1 + \lambda\Upsilon)x_1 \tag{5.9}$$

can now be integrated to give

$$x_1(\tau) = \frac{\mu}{\lambda - 1}(\lambda \mathrm{e}^{-\lambda\tau} - \mathrm{e}^{-\tau}) \tag{5.10}$$

which enables the leading order relationship between t and τ to be obtained as

$$\frac{\mu^\lambda t}{(\lambda-1)^\lambda} = \int_0^\tau \frac{\mathrm{d}s}{(\lambda \mathrm{e}^{-\lambda s} - \mathrm{e}^{-s})^\lambda}. \tag{5.11}$$

Here μ is related to θ through (3.8).

The solution (5.10) breaks down as $\tau \to (\log\lambda)/(\lambda - 1)$, which corresponds to $t \to \infty$, indicating the need for a new timescale τ_2, given by $\tau = (\log\lambda)/(\lambda - 1) + \varepsilon\tau_2$. An asymptotic expansion of (5.11) reveals

$$\mu^\lambda t \sim \frac{\lambda^{\lambda/(\lambda-1)}}{(\lambda-1)(-\varepsilon\tau_2)^{\lambda-1}} \qquad \text{as } \tau_2 \to -\infty. \tag{5.12}$$

In the new region we shall use the variables $X_1 = \varepsilon^{-1}x_1$ and $x_p = \zeta_p x_1$. From the analysis above we find that the appropriate matching conditions as $t \to \infty$ are

$$\begin{aligned} x_1 &\sim \frac{\lambda^{1/(\lambda-1)^2}}{((\lambda-1)\mu t)^{1/(\lambda-1)}} \\ \zeta_p &\sim \frac{\mu^{\lambda/(\lambda-1)}(\log\lambda)^{p-1}t^{1/(\lambda-1)}}{\lambda^{\lambda/(\lambda-1)^2}(\lambda-1)^{p-1/(\lambda-1)}}\left[\lambda\sum_{k=0}^{\infty}\frac{(-\log\lambda)^k}{(k+p-1)!} - \frac{1}{(p-1)!}\right]. \end{aligned} \tag{5.13}$$

The concentrations x_p asymptote to the constants

$$x_p \sim \frac{\mu\lambda^{-1/(\lambda-1)}(\log\lambda)^{p-1}}{(\lambda-1)^p}\left[\lambda\sum_{k=0}^{\infty}\frac{(-\log\lambda)^k}{(k+p-1)!} - \frac{1}{(p-1)!}\right] \qquad \text{for } p \geqslant 2 \tag{5.14}$$

as $\tau \to (\log\lambda)/(\lambda - 1)$.

5.3. $t = O(\varepsilon^{1-\lambda})$

The leading order equations on the second timescale $t_2 = \varepsilon^{\lambda-1}t$ implied by (5.12) are

$$\frac{\mathrm{d}X_1}{\mathrm{d}t_2} = \left(x_2 + \lambda\sum_{p=2}^{\infty}x_p\right) - \lambda X_1^\lambda \sum_{p=2}^{\infty}x_p \qquad \frac{\mathrm{d}x_p}{\mathrm{d}t_2} = 0 \qquad \text{for } p \geqslant 2 \tag{5.15}$$

and the x_p for $p \geqslant 2$ are thus given by the constants (5.14). The solution for X_1 is given by

$$t_2 = \lambda^{1/(\lambda-1)}\mu^{-1}\int_{X_1}^{\infty} \frac{\mathrm{d}u}{u^\lambda - 1 - \frac{(\lambda-1-\log\lambda)}{(\lambda-1)^2}} \tag{5.16}$$

the constant of integration being fixed by requiring $t_2 \to 0$ as $X_1 \to \infty$ (in order to match with (5.13)); (5.16) implies

$$x_1 \to \varepsilon\left(\frac{\lambda(\lambda-1)-\log\lambda}{(\lambda-1)^2}\right)^{1/\lambda} \qquad \text{as } t_2 \to +\infty. \tag{5.17}$$

5.4. $t = O(\varepsilon^{-\lambda})$

Here we have $x_1 = \varepsilon X_1$ and $x_p = \mathrm{O}(1)$ for $p \geqslant 2$, with the required timescale being $t_3 = \varepsilon^\lambda t$. The timescale of the coarse-grained model is thus different from that of the uncontracted one. We then have

$$\begin{aligned}
\varepsilon\frac{\mathrm{d}X_1}{\mathrm{d}t_3} &= x_2 - \varepsilon X_1^{\lambda+1} - \lambda X_1^\lambda \sum_{p=2}^{\infty} x_p + \lambda\sum_{p=1}^{\infty} x_{p+1} \\
\frac{\mathrm{d}x_2}{\mathrm{d}t_3} &= \varepsilon X_1^{\lambda+1} - X_1^\lambda - x_2 + x_3 \\
\frac{\mathrm{d}x_p}{\mathrm{d}t_3} &= x_{p-1}X_1^\lambda - x_p X_1^\lambda - x_p + x_{p+1} \qquad p \geqslant 3
\end{aligned} \tag{5.18}$$

the leading order solution of the first equation being

$$X_1^\lambda = 1 + \frac{x_2}{\lambda\sum_{p=2}^{\infty} x_p}. \tag{5.19}$$

As in section 4.4 the concentrations x_p cannot in general be found, but we can give the large-time asymptotic behaviour of solutions; we have $X_1 \to 1$ as $t_3 \to \infty$, together with the continuum limit of (5.18), which is the heat equation (cf (4.18)), giving

$$x(p, t_3) \sim \frac{\mu p \mathrm{e}^{-p^2/4t_3}}{2\lambda\sqrt{\pi}t_3^{3/2}} \qquad \text{as } t_3 \to \infty \qquad \text{with } p = \mathrm{O}(t_3^{1/2}). \tag{5.20}$$

5.5. $t = O(\varepsilon^{-(\lambda+1)})$

Once again, the evolution for $\lambda > 1$ occurs on a timescale different from that of the uncontracted model. Here we must take $t_4 = \varepsilon^{\lambda+1}t$, $p_4 = \varepsilon^{1/2}p$, $x_1 \sim \varepsilon + \varepsilon^{3/2}Y_1$, $x_p \sim \varepsilon X(p_4, t_4)$ for $p_4 = \mathrm{O}(1)$. To leading order this gives

$$\frac{\partial X}{\partial t_4} = \frac{\partial^2 X}{\partial p_4^2} - \lambda Y_1 \frac{\partial X}{\partial p_4} \tag{5.21}$$

for the outer solution. A similar analysis to that of section 4.5 gives the inner solution $X_p = 1$ for $p = \mathrm{O}(1)$, and $Y_1 = -1/\lambda\int_0^\infty X(p_4, t_4)\,\mathrm{d}p_4$; (5.21) is to be solved subject to $X \to 0$ as $p_4 \to \infty$ and $X = 1$ at $p_4 = 0$. The large-time behaviour is

$$X = \exp\left(-p_4\sqrt{\lambda/\mu}\right) \qquad Y_1 = -1/\sqrt{\lambda\mu} \tag{5.22}$$

which is consistent with the exact solution (3.5) with $\theta \sim 1 - \sqrt{\varepsilon/\lambda\mu}$.

The structure of the asymptotic solution is thus broadly similar to the full, uncontracted model. However, the timescales involved become longer as the mesh parameter λ is

increased. The second timescale is longer than the first for $\lambda > 1$, rather than just being a timeshift. The exact form of the distribution is also different and the expression for the distribution at the end of the second timescale is unfortunately much more complex than (4.13). Nevertheless, by the end of the third timescale ($t = \mathrm{O}(\varepsilon^{-\lambda})$) the form of the distribution has returned to the simple form of (4.19). The fourth timescale again marks the approach to equilibrium.

6. Discussion

There are several studies of steady-state solutions and closed form solutions for special initial conditions. We have given a much more general approach to the description of the large-time behaviour in the constant monomer case (with particular focus on the the evolution of clusters of large size, this being a completely new result) and of the various temporal phases that arise in the aggregation-dominated constant mass case (including several new, explicit descriptions of the intermediate asymptotic behaviour).

Our results enable us to make a quantitative comparison between the predictions of the original system and of the coarse-grained system. The results in section 5 have been presented in the unscaled time variable, leading to significant differences in the kinetics; for example, the original formulation of the problem reaches equilibrium on a timescale of $\mathrm{O}(1/\varepsilon^2)$, whereas the coarse-grained contraction equilibrates on a timescale of $\mathrm{O}(\varepsilon^{-\lambda-1})$. These differences can be corrected for by application of the rescaling (3.10). Under this choice of scaling, the full system of equations (4.2) passes through the four timescales $\hat{t} = \mathrm{O}(\varepsilon)$, $\varepsilon \log(1/\varepsilon) + \mathrm{O}(\varepsilon)$, $\mathrm{O}(1)$ and $\mathrm{O}(1/\varepsilon)$, whereas the contracted system (5.3) reacts on timescales of $\hat{t} = \mathrm{O}(\varepsilon^{\lambda})$, $\mathrm{O}(\varepsilon)$, $\mathrm{O}(1)$ and $\mathrm{O}(1/\varepsilon)$. Thus the fastest timescale is not well approximated by the coarse-grain contraction procedure, but the slower timescales can be correctly reproduced if one is careful with the choice of scaling. In the systems where the coarse-grained contraction has been used previously, there have been physical parameters in the problems suggesting a natural 'mesh size' for λ. Given the absence of a natural size-scale for λ in the models considered here, the agreement between the contracted model and the full Becker–Döring equations is encouraging. However, our asymptotic analysis has systematically shown the widespread applicability of continuum versions of the model, thereby indicating that such continuum limits are viable competitors to coarse-graining in terms of simplifying the system.

This work also sheds some light on issues of metastable solutions [9] and their evolution. At a superficial level we see that the late stages of the reaction occur on long timescales (as found by balancing in our asymptotic analysis), and these long timescales can be interpreted as a type of metastability. At a deeper level, we note that the density-conserving systems studied here have a Lyapunov function ($V(c)$) which corresponds to the free energy of the system (4.2). We now analyse the evolution of this free energy. For monodisperse initial conditions, V takes the value $\varrho \log(\varrho/e)$ at $t = 0$, dropping to $\varrho(1-1/e)\log\varepsilon$ by the end of the $t = \mathrm{O}(1)$ timescale and, to leading order, remaining at this value throughout the second timescale. By the end of the third timescale ($t = \mathrm{O}(1/\varepsilon)$), V has descended further, to $\varrho \log\varepsilon$, so its value is almost twice as large in magnitude as during the $t \sim (e/\varrho)\log(1/\varepsilon)$ timescale. Over the final, slowest timescale V does not alter at leading order, taking its equilibrium value throughout. We can identify solutions whose leading order free energy is equal to the free energy at equilibrium as being in a metastable state. A similar analysis can be carried through with the coarse-grain contracted system with similar results. For monodisperse initial conditions, $V = \varrho \log(\varrho/e)$ at $t = 0$, reducing to $\varrho(1-\lambda^{-\lambda/(\lambda-1)})\log\varepsilon$ by the end of the second timescale and to $\varrho \log\varepsilon$ by the end of the third. To leading order, it

then adopts the equilibrium value, even though the system is not at equilibrium. The system continues to converge to equilibrium over the longest timescale, during which correction terms in the Lyapunov function decrease.

The transformation in section 2.4.4 which enabled results for $\theta < 1$ to be immediately deduced from those for $\theta > 1$ can be extended to general rate constants a_r, b_r. Details of this are given in appendix B. It is hoped to extend the asymptotic results of this paper to more general reaction rates in a subsequent paper.

Acknowledgments

JADW thanks Dr Peter Coveney for many stimulating conversations and suggestions. JADW is grateful to both the Nuffield Foundation and the University of Nottingham for awards under their schemes for new lecturers. JRK gratefully acknowledges a Leverhulme Trust Research Fellowship.

Appendix A. Solutions for exponentially decaying initial data

Here we analyse the special case of polydisperse initial conditions in which the cluster size decays exponentially for large r, with $\log c_r \sim -\omega r$ as $r \to \infty$ at $t = 0$ for some constant ω.

The one-parameter family of solutions to Clairaut's equation (2.18) is

$$F(\eta) = -\omega\eta + b\mathrm{e}^{-\omega} - b - ac_1 + ac_1\mathrm{e}^{\omega}. \tag{A.1}$$

However, this holds only for

$$\eta > \eta_c(\omega) \equiv ac_1\mathrm{e}^{\omega} - b\mathrm{e}^{-\omega} \tag{A.2}$$

at $\eta = \eta_c$ the required solution switches to the envelope solution (2.19) (as is typical for Clairaut's equation, cf [11]), F and F_η being continuous at $\eta = \eta_c$. For $ac_1 - b < \eta < \eta_c$, F is given by (2.19) and the wavespeed is thus still $ac_1 - b$, with the large-time behaviour differing from that discussed in earlier sections only for $r/t > \eta_c$, where the solution is exponentially small.

Appendix B. Equivalence transformations

Our purpose here is to note some generalizations of the transformation given in section 2.4.4, treating the constant monomer case (1.2) with general kernels. Writing

$$c_r = \frac{\phi_r}{1 + Kd_r} \tag{B.1}$$

where

$$d_1 = 0 \qquad d_r = \sum_{s=1}^{r-1} \frac{1}{a_s Q_s c_1^{s+1}} \qquad \text{for } r \geqslant 2 \tag{B.2}$$

and K is an arbitrary constant, yields

$$\dot{\phi}_r = H_{r-1} - H_r \qquad H_r = \alpha_r\phi_r\phi_1 - \beta_{r+1}\phi_{r+1} \tag{B.3}$$

with

$$\alpha_r = \frac{1 + Kd_{r+1}}{1 + Kd_r}a_r \qquad \beta_r = \frac{1 + Kd_{r-1}}{1 + Kd_r}b_r. \tag{B.4}$$

The partition function for (B.3), defined by $\alpha_r \Omega_r = \beta_{r+1}\Omega_{r+1}$, $\Omega_1 = 1$, is given by

$$\Omega_r = Q_r(1 + Kd_r)^2 \tag{B.5}$$

and, defining

$$\nu_1 = 0 \qquad \nu_r = \sum_{s=1}^{r-1} \frac{1}{\alpha_s \Omega_s \phi_1^{s+1}} \qquad \text{for } r \geqslant 2 \tag{B.6}$$

we have

$$\nu_r = \frac{d_r}{1 + Kd_r}. \tag{B.7}$$

The inverse transformation is

$$\begin{aligned} &\phi_r = \frac{c_r}{1 - K\nu_r} \qquad Q_r = \Omega_r(1 - K\nu_r)^2 \qquad d_r = \frac{\nu_r}{1 - K\nu_r} \\ &a_r = \frac{1 - K\nu_{r+1}}{1 - K\nu_r}\alpha_r \qquad b_r = \frac{1 - K\nu_{r-1}}{1 - K\nu_r}\beta_r. \end{aligned} \tag{B.8}$$

If $\alpha_r = \alpha$, $\beta_r = \beta$ are constant then

$$\nu_r = \frac{1 - (\beta/\alpha\phi_1)^{r-1}}{\phi_1(\alpha\phi_1 - \beta)} \tag{B.9}$$

and a system with rate constants a_r, b_r given in terms of α and β by (B.8) is therefore mapped by this transformation into a system in which the rate constants are independent of r.

In the steady-state case

$$a_r c_1 c_r - b_{r+1} c_{r+1} = J \qquad c_r = Q_r c_1^r (1 - Jd_r) \tag{B.10}$$

we have

$$\alpha_r \phi_1 \phi_r - \beta_{r+1}\phi_{r+1} = J + K \qquad \phi_r = \Omega_r \phi_1^r (1 - (J + K)\nu_r). \tag{B.11}$$

In view of (B.11), by the choices

$$J = 1/d_\infty \qquad K = -1/d_\infty \tag{B.12}$$

and

$$J = 0 \qquad K = 1/\nu_\infty \tag{B.13}$$

we are thus able to map between the two types of time-independent solution described in section 2. If in the equilibrium solution

$$c_r = Q_r c_1^r \tag{B.14}$$

there is a critical value $c_1 = c_c$, say, such that (B.14) is of finite mass for $c_1 < c_c$ only, then it will grow exponentially in r for $c_1 > c_c$. It follows that d_∞ is bounded for $c_1 > c_c$ provided a_r does not decay exponentially in r and the transformation (B.1) takes one from the steady-state solution $c_r = Q_r c_1^r (1 - d_r/d_\infty)$ with $c_1 > c_c$ to the equilibrium solution $\phi_r = \Omega_r \phi_1^r$, as noted for the special case of constant rate coefficients in section 2.4.4; it follows from (B.7) that ν_∞ is then unbounded.

References

[1] Abramowitz M and Stegun I A 1964 *Handbook of Mathematical Functions* (New York: Dover)

[2] Ball J M, Carr J and Penrose O 1986 The Becker–Döring cluster equations: basic properties and asymptotic behaviour of solutions *Commun. Math. Phys.* **104** 657–92

[3] Becker R and Döring W 1935 Kinetische behandlung der Keimbildung in ubersattigten dampfern *Ann. Phys.* **24** 719–52

[4] Brilliantov N V and Krapivsky P L 1991 Non-scaling and source-induced scaling behaviour in aggregation models of movable monomers and immovable clusters *J. Phys. A: Math. Gen.* **24** 4787–803

[5] Coveney P V and Wattis J A D 1996 Analysis of a generalized Becker–Döring model of self-reproducing micelles *Proc. R. Soc.* A **452** 2079–102

[6] Coveney P V and Wattis J A D 1998 Analysis of a generalized Becker–Döring model of self-reproducing vesicles *J. Chem. Soc. Faraday Trans.* **102** 233–46

[7] Hounslow M J 1990 A discretized population balance for continuous systems at steady state *AIChE J.* **36** 106–16

[8] Hounslow M J, Ryall R L and Marshall V R 1988 A discretized population balance for nucleation, growth and aggregation *AIChE J.* **34** 1821–32

[9] Penrose O 1995 Metastable decay rates, asymptotic expansions, and analytic continuation of thermodynamic functions *J. Stat. Phys.* **78** 267–83

[10] Penrose O and Lebowitz J L 1976 *Studies in Statistical Mechanics VII: Fluctuation Phenomena* ed E Montroll and J L Lebowitz (Amsterdam: North-Holland) pp 322–75

[11] Piaggio H T H 1952 *An Elementary Treatise on Differential Equations and their Applications* revised edn (London: Bell and Hyman)

[12] Shneidman V A 1995 Theory of time-dependent nucleation and growth during a rapid quench *J. Chem. Phys.* **103** 9772–81

[13] Slezov V V, Schmelzer J and Tkatch Ya Y 1996 Number of clusters formed in nucleation-growth processes *J. Chem. Phys.* **105** 8340–51

[14] Wall S N and Aniansson G E A 1980 Numerical calculations on the kinetics of stepwise micelle association *J. Phys. Chem.* **84** 727–36

[15] Wattis J A D and Coveney P V 1997 General nucleation theory with inhibition for chemically reacting systems *J. Chem. Phys.* **106** 9122–40